Article

Time, Space, and Spectrally Resolved Studies on J-Aggregate Interactions in Zeolite L Nanochannels

Michael Busby, Christian Blum, Marc Tibben, Sandra Fibikar, Gion Calzaferri, Vinod Subramaniam, and Luisa De Cola

J. Am. Chem. Soc., **2008**, 130 (33), 10970-10976 • DOI: 10.1021/ja801178p • Publication Date (Web): 29 July 2008

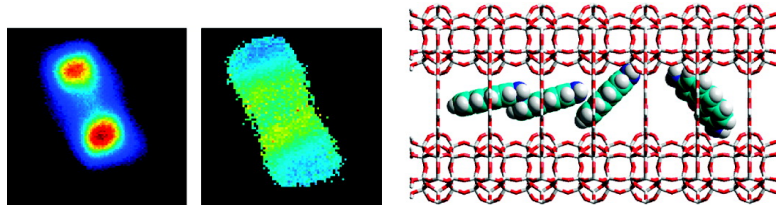

J|A|C|S
ARTICLES

Published on Web 07/29/2008

Time, Space, and Spectrally Resolved Studies on J-Aggregate Interactions in Zeolite L Nanochannels

Michael Busby,*,† Christian Blum,‡ Marc Tibben,‡ Sandra Fibikar,† Gion Calzaferri,§ Vinod Subramaniam,*,‡ and Luisa De Cola*,†

Physikalisches Institut and Center for Nanotechnology, CeNTech, University of Münster, Mendelstrasse 7, 48149 Münster, Germany, Biophysical Engineering Group, Faculty of Science and Technology and MESA+ Institute for Nanotechnology, University of Twente, 7500 AE Enschede, The Netherlands, and Department of Chemistry and Biochemistry, University of Bern, Freiestrasse 3, 3012 Bern, Switzerland

Received February 16, 2008; E-mail: busby.michael1@gmail.com; V.Subramaniam@tnw.utwente.nl; decola@uni-muenster.de

Abstract: Temporally and spectrally resolved confocal microscopy has been used to explore the behavior of pyronine intercalated zeolite L crystals at different loadings. The low pyronine loading of 0.6% exhibits photophysical behavior similar to that of the free molecule in solution, indicating molecules are isolated from each other in the crystal channels. The higher loading of 20% results in a dye gradient along the channel axis, and the presence of an additional red-shifted spectroscopic transition, with shorter lifetimes. The new band is assigned to an inline arrangement of the molecules undergoing a J-aggregate-type coupling, a process so far not observed in subnanometer channels.

Introduction

Organization of functional molecules into nano- and subnanoscale scaffolds is an appealing methodology toward the realization of highly structured systems that exploit a defined molecular geometrical control. Inorganic frameworks, such as zeolites, exhibit internal channels on the subnanometer level as well as crystalline structure and well-defined morphologies, which can be tuned between the micro- and nanoscales. Their general applications in photonics and optoelectronics, cover nonlinear optics,[1–3] microlasers,[4] light harvesting,[5] electroluminescent devices,[6] and charge separation.[7] Fundamental questions are still being asked about how the intercalated molecules diffuse,[8] organize,[9] react,[10] and interact with each other inside their scaffolds. Zeolite L possesses a crystalline structure and one-dimensional channels, making it an appealing host for organizing highly fluorescent dyes (Figure 1a). Its channels have an entrance diameter of 7.1 Å, a maximum cage diameter of 12.6 Å, and a single unit cell length of 7.5 Å, and their center-to-center distance is 18.4 Å. On the basis of its one-dimensionality, space restrictions are more severe in zeolite L than in zeolite X or Y. Pyronine (Py) and oxonine (Figure 1b) zeolite L systems are ideal for fundamental studies in unidirectional energy transfer[5] as well as applications in highly fluorescent self-assembling microobjects.[11–13] It is accepted that the above-mentioned dye molecules are individually aligned at defined angles[14] and may not slide over or stack on top of each other, thus preventing excimer[15] and H-aggregates[5] formation. It has been shown that smaller, neutral molecules may interact inside the channels leading to excimer emission.[16] Interestingly, the "end to end" alignment of molecules like pyronine and oxonine can be envisaged to result in J-aggregate-type coupling, a phenomenon so far unreported. Observing and understanding such excitonic coupling in one-dimensional channel systems is of considerable scientific interest.[17–21] Excited state lifetime

† CeNTechUniversity of Münster.
‡ University of Twente.
§ University of Bern.

(1) Cox, S. D.; Gier, T. E.; Stucky, G. D.; Bierlein, J. *J. Am. Chem. Soc.* **1988**, *110*, 2986–2987.
(2) Kim, H. S.; Lee, S. M.; Ha, K.; Jung, C.; Lee, Y. J.; Chun, Y. S.; Kim, D.; Rhee, B. K.; Yoon, K. B. *J. Am. Chem. Soc.* **2004**, *126*, 673–682.
(3) Marlow, F.; Caro, J.; Werner, L.; Kornatowski, J.; Daehne, S. *J. Phys. Chem.* **1993**, *97*, 11286–11290.
(4) Vietze, U.; Krauss, O.; Laeri, F.; Ihlein, G.; Schuth, F.; Limburg, B.; Abraham, M. *Phys. Rev. Lett.* **1998**, *81*, 4628–4631.
(5) Calzaferri, G.; Huber, S.; Maas, H.; Minkowski, C. *Angew. Chem., Int. Ed.* **2003**, *42*, 3732–3758.
(6) Alvaro, M.; Cabeza, J. F.; Corma, A.; Garcia, H.; Peris, E. *J. Am. Chem. Soc.* **2007**, *129*, 8074–8075.
(7) Garcia, H.; Roth, H. D. *Chem. Rev.* **2002**, *102*, 3947–4007.
(8) Jung, C.; Hellriegel, C.; Platschek, B.; Wohrle, D.; Bein, T.; Michaelis, J.; Brauchle, C. *J. Am. Chem. Soc.* **2007**, *129*, 5570–5579.
(9) Minoofar, P. N.; Dunn, B. S.; Zink, J. I. *J. Am. Chem. Soc.* **2005**, *127*, 2656–2665.
(10) Roeffaers, M. B. J.; Sels, B. F.; Uji-i, H.; Blanpain, B.; L'Hoest, P.; Jacobs, P. A.; De Schryver, F. C.; Hofkens, J.; De Vos, D. E. *Angew. Chem., Int. Ed.* **2007**, *46*, 1706–1709.
(11) Popovic, Z.; Otter, M.; Calzaferri, G.; De Cola, L. *Angew. Chem., Int. Ed.* **2007**, *46*, 6188–6191.
(12) Busby, M.; De Cola, L.; Kottas, G. S.; Popovic, Z. *MRS Bull.* **2007**, *32*, 556–560.
(13) Popovic, Z.; Busby, M.; Huber, S.; Calzaferri, G.; De Cola, L. *Angew. Chem., Int. Ed.* **2007**, *46*, 8898–8902.
(14) Megelski, S.; Lieb, A.; Pauchard, M.; Drechsler, A.; Glaus, S.; Debus, C.; Meixner, A. J.; Calzaferri, G. *J. Phys. Chem. B* **2001**, *105*, 25–35.
(15) Ramamurthy, V.; Sanderson, D. R.; Eaton, D. F. *J. Am. Chem. Soc.* **1993**, *115*, 10438–10439.
(16) Hashimoto, S.; Hagiri, M.; Matsubara, N.; Tobita, S. *Phys. Chem. Chem. Phys.* **2001**, *3*, 5043–5051.
(17) Ohno, O.; Kaizu, Y.; Kobayashi, H. *J. Chem. Phys.* **1993**, *99*, 4128–4139.
(18) Kobayashi, T. *J-Aggregates*; World Scientific: Singapore, 1996.
(19) Da Como, E.; Loi, M. A.; Murgia, M.; Zamboni, R.; Muccini, M. *J. Am. Chem. Soc.* **2006**, *128*, 4277–4281.

 10.1021/ja801178p CCC: $40.75

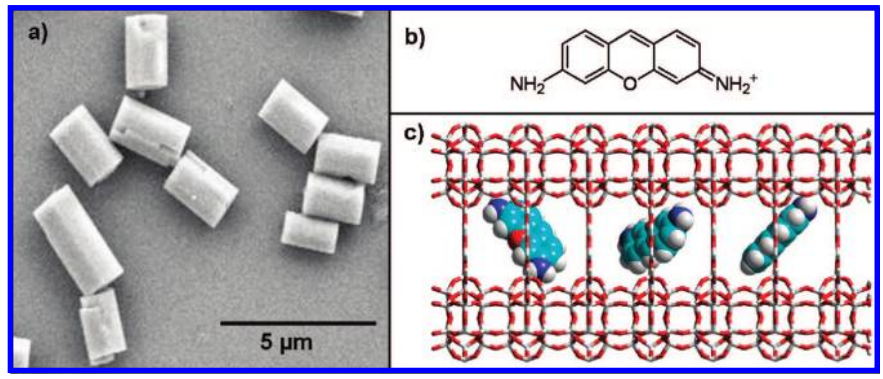

Figure 1. (a) Scanning electron microscope image of the 3 μm zeolite samples used in this study; (b) chemical structure of the cationic pyronine (Py) molecule; (c) space filling model of the isolated Py molecules in zeolite nanochannels.

studies on Py intercalated zeolite L have shown loading-dependent multiexponential decays[22] indicating that the molecules may interact with each other or the environment, though experimental evidence is still confined to bulk samples. So far, a few pioneering examples of spatially resolved analysis of single microcrystals at the diffraction limit exist,[23,24] but the full potential has not been reached. With the ultimate aim of developing a device system that exploits intermolecular excitonic interactions, we report the first example of J-aggregate coupling between dye molecules in subnanometer one-dimensional nanochannels, using advanced single crystal fluorescence lifetime and spectrally resolved confocal microscopy.

Experimental Details

Bulk Spectroscopy. All spectroscopic measurements were carried out in solutions or suspensions of spectroscopic grade methanol in 10 mm quartz cuvettes at low concentrations (less than 0.5 mg/ml). Steady-state emission spectra were recorded on a HORIBA Jobin-Yvon IBH FL-322 Fluorolog 3 spectrometer equipped with a 450 W xenon arc lamp, double grating excitation and emission monochromators (2.1 nm/mm dispersion; 1200 grooves/mm), and a TBX-4-X single-photon-counting detector. Emission spectra were corrected for source intensity (lamp and grating) and emission spectral response (detector and grating) by standard correction curves. Time-resolved measurements were performed using the time-correlated single-photon counting (TCSPC) option on the Fluorolog 3. A light emitting diode (NanoLED, 431 nm; fwhm $<$ 750 ps) with a repetition rate of 1 MHz was used to excite the sample. The excitation sources were mounted directly on the sample chamber at 90° to the monochromator. Signals were processed using an IBH DataStation Hub photon counting module and data analysis was performed using the commercially available DAS6 software (HORIBA Jobin Yvon IBH).

Microscopy. The emission from individual Py loaded zeolite crystals was characterized using a custom-built setup capable of wide field fluorescence imaging as well as scanning stage confocal microscopy for fluorescence lifetime and spectral imaging. Light sources used were a mercury lamp for wide field fluorescence imaging and a pulsed laser diode emitting at 469 nm (BDL475, Becker & Hickl, Germany) for local excitation when recording lifetimes and emission spectra. The sample was illuminated using a 100× objective (100×, 1.4 NA oil, UPlanSapo, Olympus), and the emission from the sample was collected by the same objective. Wide field images were recorded with a color camera (AxioCam HRc, Zeiss). For the emission images a standard blue filter cube (U-MWB2, Olympus) was used. White balance was optimized for a halogen light temperature of 3200 K in accordance with the manufacturer's recommendation for fluorescence imaging. We verified the consistency between the color camera image and the coloring visible via the eyepiece of the microscope. Contrast, brightness and gamma were globally optimized for the whole images, and no digital color changing filters were applied. To highlight color variations barely visible in the true color images false color images were calculated by separating the RGB values from the image files and dividing the red channel by the green channel after applying a threshold to account for noise and background signal. When a laser for confocal imaging was used, the filtercube was replaced by a glass plate as beam splitter and a long pass filter (RazorEdge 473.0 nm, Semrock) to block reflected and scattered excitation light. For fluorescence lifetime imaging a time correlated single photon counting (TCSPC) module (SPC-830, Becker & Hickl, Germany) attached to a single photon avalanche diode detector (PDM Series, MPD, Italy) was used. The lifetime data was analyzed using the Becker & Hickl SPCImage software package. Binning values of 0 were used in all cases to maximize resolution, except for the measurement involving the 640−700 nm band-pass filter; here a binning of 1 was required for higher photon counts. To record local emission spectra, emitted light was imaged via a prism spectrometer onto a cooled CCD camera (Newton EMCCD DU970N−BV, Andor). Wavelength calibration was achieved using a calibrated light source (Cal-2000 Mercury Argon Calibration source, Ocean Optics).

Zeolite L Synthesis. Zeolite L crystals were synthesized as published previously.[25] Potassium hydroxide (Fluka, pellets ≥86%), sodium hydroxide (Merck, pellets ≥99%) and aluminum hydroxide (Riedel-de Haën, powder purum) were diluted in bidistilled water. To this solution a silica suspension (Evonik Degussa AeroDisp W 1226) was added under vigorous stirring to obtain a white gel with the following composition 3 Na_2O:9.6 Si_2O:1 Al_2O_3:158.6 H_2O. The gel was transferred into a Teflon vessel that was sealed and put into an oven for 144 h at 160 °C. The obtained white solid was exchanged with 0.1 M KNO_3 and washed several times with bidistilled water and dried. The product was characterized with XRD, SEM, and EDX.

Zeolite Intercalation. Zeolites were cation exchanged upon heating to 80 °C in the presence of an aqueous solution of Py for a period of 36 h. Samples were dispersed and centrifuged repeatedly from methanol, to remove free dye absorbed on the crystal surface.

(20) Del Caño, T.; Duff, J.; Aroca, R. *Appl. Spectrosc.* **2002**, *56*, 744–750.
(21) Del Caño, T.; Hashimoto, K.; Kageyama, H.; De Saja, J. A.; Aroca, R.; Ohmori, Y.; Shirota, Y. *Appl. Phys. Lett.* **2006**, *88*, 071117.
(22) Yatskou, M. M.; Meyer, M.; Huber, S.; Pfenniger, M.; Calzaferri, G. *ChemPhysChem* **2003**, *4*, 567–587.
(23) Pauchard, M.; Huber, S.; Meallet-Renault, R.; Maas, H.; Pansu, R.; Calzaferri, G. *Angew. Chem., Int. Ed.* **2001**, *40*, 2839–2842.
(24) Hashimoto, S.; Uehara, K.; Sogawa, K.; Takada, M.; Fukumura, H. *Phys. Chem. Chem. Phys.* **2006**, *8*, 1451–1458.
(25) Zabala Ruiz, A.; Bruehwiler, D.; Ban, T.; Calzaferri, G. *Monatsh. Chem.* **2005**, *136*, 77–89.

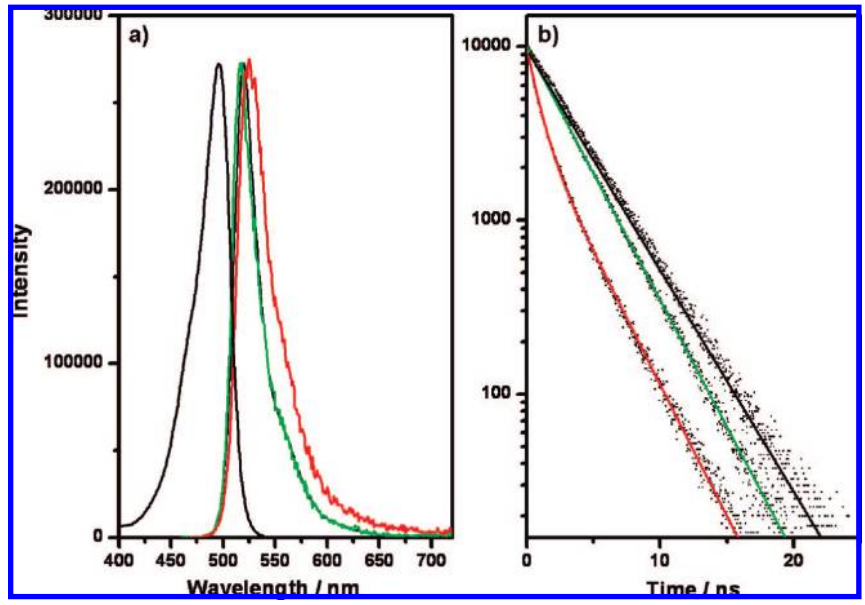

Figure 2. (a) Absorption of Py in MeOH, emission spectra ($\lambda_{ex} = 470$ nm) of Py in MeOH (black), 0.6% Py−zeolite L (green), and 20% Py−zeolite L (red) suspended in MeOH. (b) Monoexponential and biexponential lifetime decay traces and fits for Py in MeOH, $\tau = 3.6$ ns (black), 0.6% Py−zeolite L, $\tau = 2.9$ ns (green), and 20% Py−zeolite L, $\tau_1 = 2.4$ ns (61%) and $\tau_2 = 0.7$ ns (39%) (red) suspended in MeOH. $\lambda_{ex} = 431$ nm, λ_{em}=550 nm, excitation pulse fwhm < 200 ps.

In the case of the sample corresponding to 20% loading, a second identical intercalation was performed. Loading assays were performed by dissolving a known mass of crystals in HF and measuring the absorption spectrum of the free dye, thus calculating their concentration.[14] (% Loading = no. molecules/no. sites, where no. sites = no. unit cells/2.)

Results

Zeolite L samples (3 μm long) were intercalated with Py at concentrations of 0.6% and 20% via ion exchange. Bulk fluorescence spectra of the 0.6% Py sample were measured in a methanol suspension, with an excitation wavelength of 470 nm. Emission spectra mirror that of the absorption with a maximum at 518 nm which decreases in intensity through the vibronic progression up to 650 nm.

These spectral features are identical to those observed for the free Py molecules in methanol solutions (Figure 2a). The 20% sample, interestingly, had the emission band shifted to 525 nm, see Figure 2a. Variation in excitation wavelength gave no dramatic changes in the emission spectra, and samples measured as drop cast films also gave similar results, albeit with a slightly more intense shoulder between 600−675 nm for the 20% sample. The shift in band maximum may be attributed to reabsorption of emitted photons in the 20% crystals.

Fluorescence lifetimes for all samples were measured upon excitation at 431 nm and emission at 550 nm and are shown in Figure 2b. The free Py molecule in methanol could be easily fitted to a monoexponential decay function with a characteristic decay time of 3.6 ns. The 0.6% loading also shows a monoexponential decay, although the excited-state is reduced in lifetime from 3.6 to 2.9 ns. In contrast the 20% samples show biexponential kinetics of $\tau_1 = 2.4$ ns and $\tau_2 = 0.7$ ns (39%), see Figure 2b. These results agree well with those reported, for loaded pyronine zeolites, previously.[22]

To further analyze and quantify the inhomogeneities observed in bulk, the crystals were investigated with a conventional epifluorescence microscope using a standard filtercube for true color imaging above 510 nm (see Figure 3). All crystals showed a distinctive green emission. Interestingly, the 0.6% samples showed a homogeneous filling over the whole length of the crystals, whereas the 20% samples had the emission intensity decreasing toward the middle of the crystals.[26] The higher loaded crystals showed a hardly noticeable yellow tinge in the true color images, which could be confirmed by analyzing the RGB channels of the cameras output file. To quantify the amount of high vs low wavelength emission we calculated the ratio of the red camera channels to the green channels as can be seen in Figure 3b,d. A stronger red contribution to the crystal emission is localized on the ends, a spectral feature which would correspond to the weak shoulder seen between 600−675 nm in the bulk samples. The 0.6% samples possess a clean green emission profile. A correlation between the microscopic appearance, loading, spectra, and lifetime of the crystals was beginning to appear.

The averaging effects of bulk spectroscopy, in combination with the evident variations in loading patterns and colors seen under the epifluorescence microscope, complicate the understanding of the photophysics of the Py−zeolites on the submicrometer scale. Single crystals of the 0.6% Py−zeolite L sample were chosen and analyzed with a custom-built confocal microscope capable of lifetime and spectral imaging. Each crystal was imaged twice, once recording decay curves and once for recording the emission spectrum from each sampled point of the crystal. Three spectra taken at the middle and both ends of a crystal are displayed in Figure 3e. The intensity map of a representative crystal and the cross section across which the spectra were measured are shown in Figure 4a. The homogeneous filling of the crystals is confirmed by this measurement. Spectra showed a maximum at 518−520 nm and are similar in shape to the bulk measurements and that of the free Py molecule in solution. No variations in spectral shape were observed throughout the crystal. Fluorescence lifetime maps were recorded with a stepsize of 200 nm. The measured decay

(26) Hashimoto, S.; Moon, H. R.; Yoon, K. B. *Microporous Mesoporous Mater.* **2007**, *101*, 10–18.

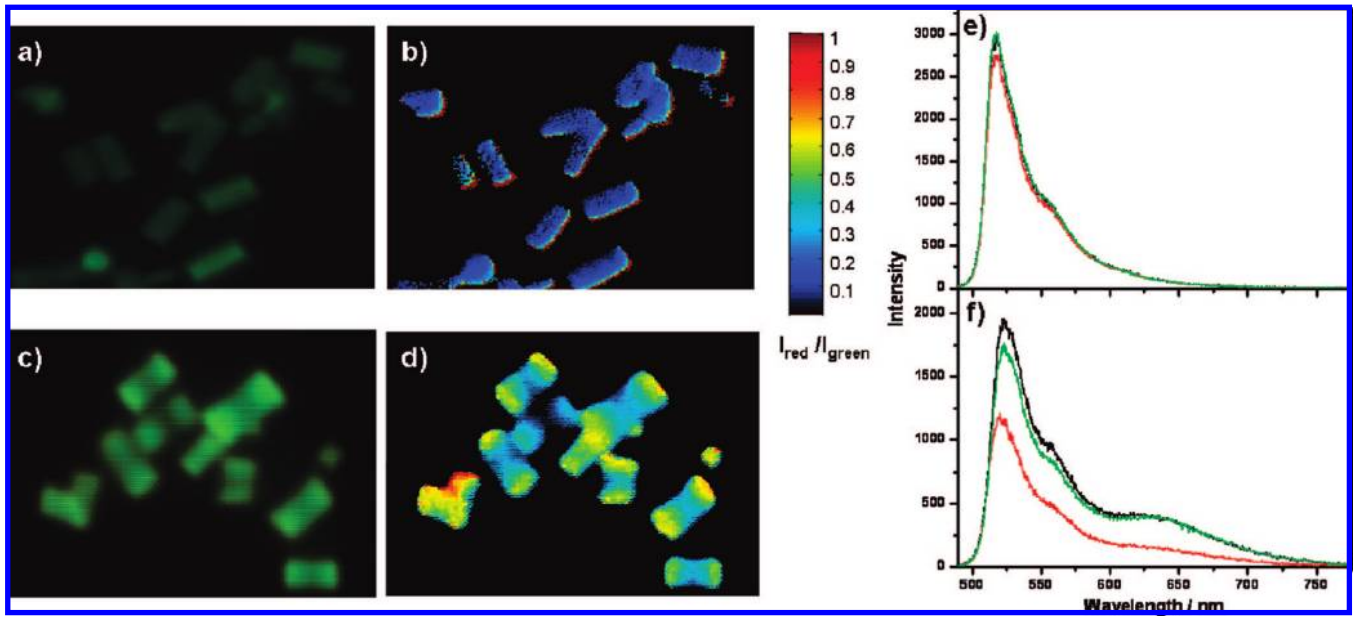

Figure 3. Epifluorescence micrographs of the Py−zeolite L samples at 0.6% (a) and 20% (c) loading. False color images of the red channels divided by the green channel at 0.6% (b) and 20% (d) loading, highlighting the larger contribution of emission above 600 nm that results in the yellow tinge in the 20% crystal. Confocal point spectra of a single crystal, for 0.6% (e) and 20% (f) loading taken at the ends (black, green) and middle (red) of the crystal. The presence of a new band can be seen on the ends of the 20% sample. The cross sections are depicted in Figure 4. The average crystal size is 3 μm.

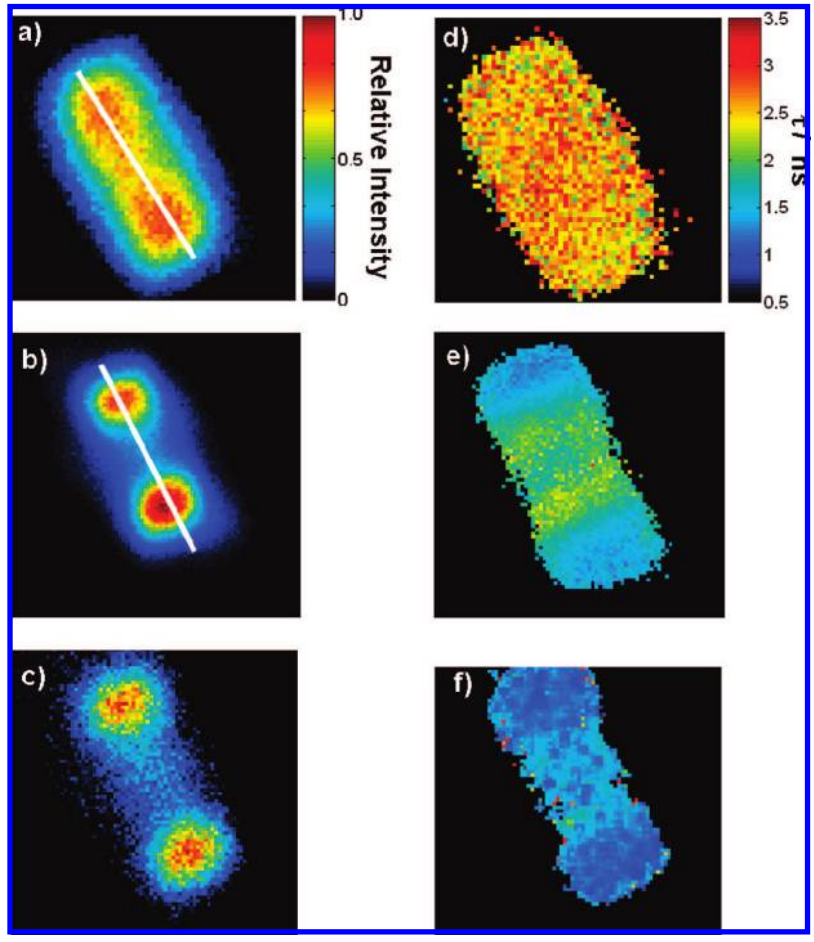

Figure 4. Normalized confocal intensity images of the (a) 0.6%, (b) 20%, and (c) 20% measured with a 640−700 nm band-pass filter, Py−zeolite L crystals. Corresponding fitted monoexponential lifetime images of the (d) 0.6%, (e) 20%, and (f) 20% measured with a 640−700 nm band-pass filter, Py−zeolite L crystals. Scan areas are 3 × 3 μm for 0.6% loading, 4 × 4 μm for 20% loadings. Cross sections shown in a and b correspond to the regions were the single point spectra in Figure 3e,f were measured. The average crystal size is 3 μm.

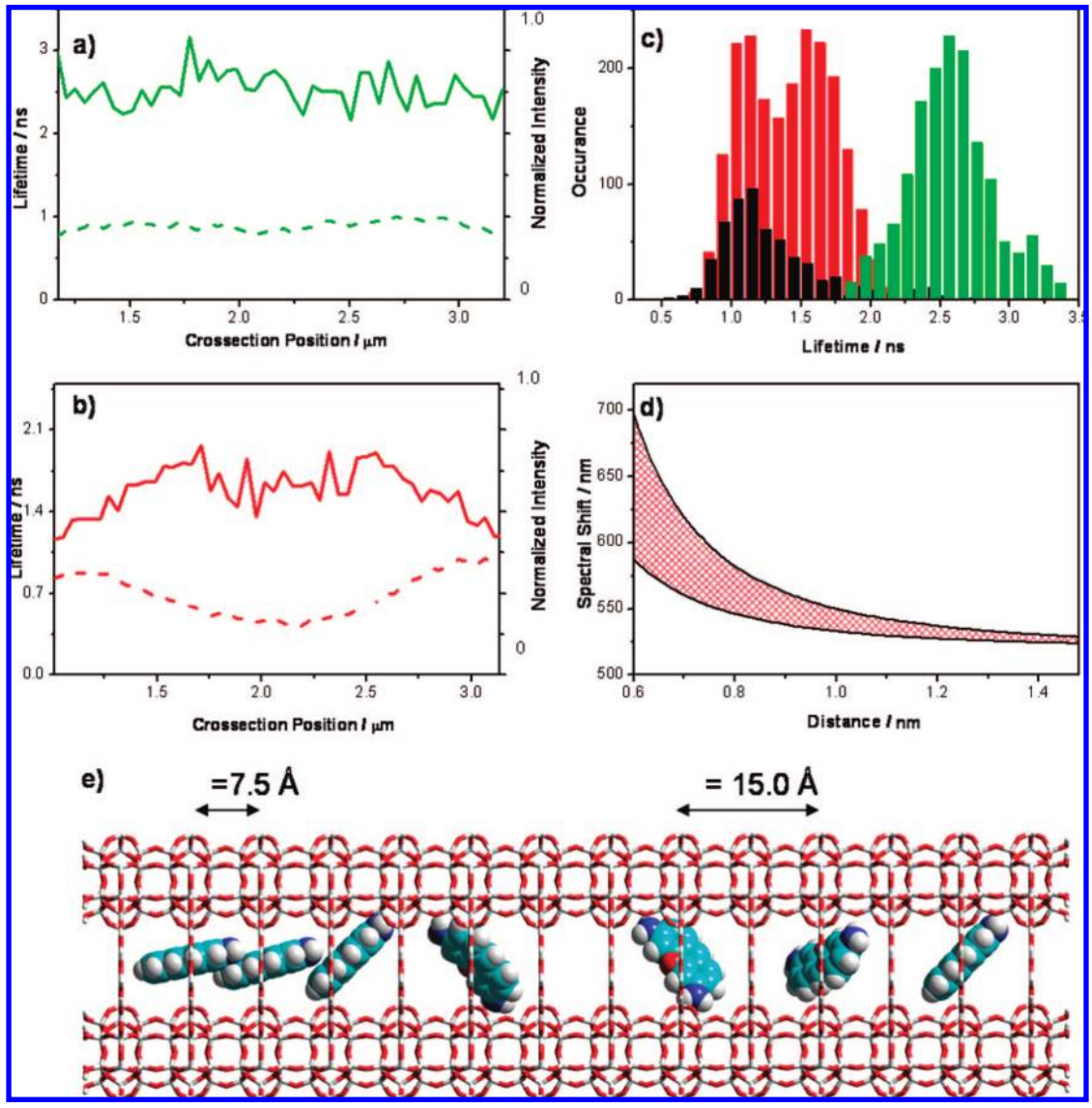

Figure 5. Variations in lifetime (solid line) and normalized intensity (dashed line) along the cross section of the single (a) 0.6% zeolite L crystal and (b) 20% zeolite L. (c) Monoexponential lifetime distribution histogram of the single Py−zeolite L crystal, shown in Figure 4 at 0.6% loading (green), 20% loading (red), and 20% loading, measured with a 640−700 nm band-pass filter (black). (d) Calculated spectral shift in nm between two Py molecules undergoing excitonic coupling, as a function of their center to center distance. We show the range of the spectral shift in the interval of refractive indexes between 1 and 1.49 by the top and bottom curves, respectively. (e) Molecular models of two different packing densities of Py in zeolite L channels.

characteristics fitted well to a monoexponential decay function. Biexponential fits neither improved χ^2 nor provided significant new lifetime components within the continuity of a single crystal (decay traces, fits, and single point spectrum are shown in the Supporting Information). There were no regional variations in lifetime across the crystal cross section, Figure 5a. The lifetime distribution histogram of the presented crystal had a maximum value at 2.6 ns, see Figure 5c, well in the range of the measured averaged bulk lifetime of 2.9 ns.

The 20% Py−zeolite L samples were subject to an identical procedure of measurement. In Figure 4b,e we present one data set of a representative crystal. The confocal intensity map displays a gradient of intensity, varying from its maximum at the plane of the channel entrances and decreasing by about 50% toward the middle of the crystal. On the basis of the bulk average loading we can say that the ends of the crystals will have a local concentration significantly greater than 20%, and vice versa for the center. The spectral imaging across the cross section shows a direct correspondence toward the intensity gradient. The low concentration center of the crystal gives rise to an emission spectrum with a band maximum at 520 nm similar to that observed in the bulk spectrum. A weak and broad shoulder is seen between 600−700 nm. Toward the highly concentrated ends, the band maximum is again seen at 520 nm but a new band is present at 630 nm. There is a direct correlation between the absolute emission intensity and that of the 630 nm band, see Figure 3f. The 630 nm band intensity was seen to be particularly strong on crystals that were standing on their ends exposing the highly concentrated bases.

Lifetime imaging was performed to shed light on the origins of the new 630 nm band. The recorded decay curves obtained for each pixel in the lifetime image of single crystals could again be well fitted to monoexponential decay (decay traces, fits, and single point spectrum are shown in the Supporting Information). It must be noted that although at each pixel a monoexponential function gives the best fits, in fact biexponential fits would typically result in τ_2 values that had either comparable lifetimes or amplitudes of less than 10%. This might be explained by

taking into account that what we are measuring may represent the major visible component in a nanoenvironment where multiple decay processes are present. The lifetime variations seen over the entire crystal indicate the existence of different nanoenvironments due to different local concentrations.[15,22] At the ends of the crystals, the emission decays shorten to around 1 ns, while toward the middle a clear increase is seen up to 2 ns. The lifetime distribution of a single crystal is broader than that observed in the 0.6% sample and presents two maxima, at 1.2 and ~1.7 ns (see Figure 5c). On the basis of the lifetime image, these two populations can be assigned to the ends and the middle of the crystal, respectively. Between these two extremes the lifetime follows an inverse relationship to the intensity, which can be best visualized in a plot of the intensity (solid line) and lifetime (dashed line) along the central longitudinal axis of the crystal (see Figure 5b). These two lifetime populations correspond to the biexponential decay seen in the bulk measurements. The above-mentioned lifetimes correspond to emission measured from the long pass filter at 475 nm to the detectors limit at beyond 900 nm and thus contain components from both the 520 and 630 nm bands. Measurements were repeated with a 640−700 nm band-pass filter to collect emission only from the 630 nm band. Photon counts were significantly lower than before, although the zeolite crystal could be visualized and monoexponential decays fitted. The majority of emission was located at the ends of the crystals, with the center being almost devoid of emission (see Figure 4c). The lifetime histogram of the single crystal follows a single distribution with a maximum around ~1.2 ns (see Figure 5c) (decay traces, fits, and single point spectrum are shown in the Supporting Information). This lifetime corresponds well to the fast component seen in the full color experiment. The same lifetime is seen all over the crystal ends. The single crystal chosen was representative of the sample and displayed an inhomogeneity in loading which corresponded to a broad distribution of lifetimes, where the regions of higher loading possessed faster decays.

Discussion

Both bulk and single crystal experiments show the 0.6% Py zeolites to behave as the free Py molecule in solution, with similar spectral shapes and energies, though with slightly reduced lifetimes. The single crystal experiments confirm that there are no local variations in spectra or lifetime. Single exponential kinetics were fitted in all cases, indicating that there are no major variations in the local environments around the emissive molecules.

A more complex picture is presented in the 20% loading case. Samples displayed variations in emission intensity, corresponding to variations in dye concentration, and an inverse relation with the fluorescence lifetime. Interestingly, regions of highest loading gave rise to a second, red-shifted spectroscopic transition at 630 nm possessing a lifetime of 1.2 ns. This fast decay corresponds to the 0.7 ns decay component seen in the multiexponential bulk lifetime measurements. Similarly the region of lowest loading has a longer-lived population with a lifetime approaching 2 ns, again related to the longer component of 2.4 ns seen in the bulk measurements. It must be noted that the average single crystal lifetimes are consistently lower, by a few hundred picoseconds, than those measured on the bulk apparatus, possibly a result of the difference in instrumental setup. Such behavior is dramatically different from the sample with low loading and indicates that the intercalated molecules are experiencing differing environments.

Reabsorption or radiative energy transfer process cannot be ruled out and are thought to result in the shift in absorption maxima between the band maxima of the 0.6 and 20% loaded samples, from 518 to 525 nm. Importantly, the blue part of the emission spectrum, close to the absorption overlap is thought to be solely affected.[27] This is supported by quantitative modeling of the expected spectral changes caused by self-absorption. Studies of the Py molecule in solution at low and high concentrations also confirm the expected increase in decay lifetime that result from high concentrations.[28] Although reabsorption processes are present, the trend toward shorter lifetime in regions of higher concentration are in contrast to the expected increase in lifetime, thus ruling it out as a cause of the shorter lifetimes and most importantly the novel band at 630 nm. Homo-FRET or energy migration between Py molecules is also not thought to be a significant effect, as no changes in lifetime are expected from this process.[29–31] Similarly, photonic processes such as the influence of lifetime induced by the dielectric of the medium can be excluded owing to the use of index matching immersion oil to cover the zeolites.[32]

Excimers in the supercages of zeolites X and Y have been observed for neutral molecules such as pyrene, perylene, and anthracene at low concentrations.[24,33–35] The interaction involves the face to face stacking of the molecules in close proximity, an arrangement possible because of the three-dimensional supercages. Excimers have been observed for anthracene in Zeolite L, based on a linear arrangement of the molecules.[16] For all of these molecules, excimer formation is readily observed in solution, and their small size allows for stacking in the zeolite pores. No evidence for excimer formation for cationic xanthene dyes exists in solution. Xanthene dyes have been shown to form H aggregates in solution, though the low energy emission is forbidden. This interaction is prevented once the dyes enter the channels of zeolite L and emission from isolated molecules is observed.[5] The influence of zeolite dimensionality has been elegantly proven by Ramamurthy by comparing the intercalation of a similar xanthene dye thionine into zeolite L and Y.[15] H aggregates were present only in zeolite Y, which result in quenched emission. Molecules behave as isolated entities in zeolite L. Furthermore, geometrical constraints make the face-to-face stacking of molecules in a single unit cell of zeolite L at comparable and low concentrations, quite improbable. Interestingly, studies on the intercalation of Py into zeolite L at a loading of 0.06% have shown that the molecules align themselves at an angle of 72° between two unit cells.[14] On the basis of the geometrical impossibility of excimers and H aggregates being formed, an alternative is J-type aggregate coupling, which results from an inline arrangement of the molecules transition dipoles that undergo an exciton coupling.[36,37] Equation 1 describes the magnitude of interaction β_c caused by

(27) Katoh, R.; Sinha, S.; Murata, S.; Tachiya, M. *J. Photochem. Photobiol., A* **2001**, *145*, 23–34.
(28) Valeur, B. *Molecular Fluorescence: Principles and Applications*; Wiley-VCH: Weinheim, Germany, 2002.
(29) Förster, T. *Annal. Phys.* **1948**, *6*, 55.
(30) May, V.; Kühn, O. In *Charge and Energy Dynamics in Molecular Systems*; Wiley-VCH: Weinheim, Germany, 2004.
(31) Lutkouskaya, K.; Calzaferri, G. *J. Phys. Chem. B* **2006**, *110*, 5633–5638.
(32) Schniepp, H.; Sandoghdar, V. *Phys. Rev. Lett.* **2002**, 89.
(33) Ramamurthy, V. *Photochemistry in Organized and Constrained Media*; VCH: New York, 1991.
(34) Thomas, J. K. *Chem. Rev.* **2005**, *105*, 1683–1734.
(35) Liu, X.; Iu, K. K.; Thomas, J. K. *J. Phys. Chem.* **1989**, *93*, 4120–4128.

J-aggregate coupling from which the spectral shift can be derived. Important parameters are the oscillator strength *f*, (0.66) for Py, from which the electronic transition dipole moment μ_{AA^*} can be calculated, the distance between the two molecules *R,* their relative orientation toward each other described as κ_{A^*A}, and the refractive index of the medium *n*. A refractive index interval between 1 and 1.49 has been used to illustrate the range of values possible. We assume that the refractive index of water which is equal to 1.33 would be a reasonable choice because the cosolvent inside of the channels of the material we have investigated is water; 1.49 is the refractive index of zeolite L. The calculation results are illustrated in Figure 5d).

$$\beta_c = \frac{1}{4\pi\varepsilon_0 n^2}\frac{|\mu_{AA^*}|^2}{R^3}\kappa_{A^*A} \quad (1)$$

Typically J-aggregate coupling results in absorption and emission bands at lower energy than the monomer and decay with a faster lifetime,[18] characteristics that are indeed present in our measurements. Furthermore, the new luminescence band is seen in regions of highest loading, where the probability of achieving a dense packing is highest. The new red-shifted aggregates may also act as an energy acceptor from the isolated Py molecules. This energy transfer from isolated Py molecules to Py−J aggregates results in a reduced lifetime for isolated Py molecules acting as energy transfer donor. This process may additionally explain, for the 20% sample, the short excited-state lifetime measured in the center of the crystal, which quenches, even in the low-loaded region, the fluorescence of the pyronine, see Figure 4e. The packing of Py in the zeolite channels is visualized in Figure 5e, which shows high packing on the left, where the dyes come so close that J-aggregate coupling can become significant. At a distance of 7.0 Å, calculations predict shifts up to ~60 nm and a decrease of lifetime by a factor of 2, at a refractive index of the medium of 1.33. These values fit well to our experimental observations for the 20% loading, and provides a theoretical argument for the presence of J-aggregate coupling in the zeolite L nanochannels. The Py molecules on the right of Figure 5e span two unit cells each, with a cone angle of 72°. Here, the center to center distance between two molecules is about 15 Å. Interaction energy is low in this case, and any corresponding band splitting is expected to be very small. This is the arrangement based on low zeolite loadings and has been confirmed by detailed polarization studies.[14] The lack of aggregates is seen in the monoexponential decay kinetics and spectra that correspond to the free molecule. The low absolute concentration of the aggregates explains its near invisibility in the bulk spectra, where it is masked by the monomer emission.

Conclusions and Outlook. J aggregates are typically seen in the solid state in porphyrins,[17] cyanine dyes,[18] and more recently in oligophenylvinylenes, oligothiophenes,[19]and perylenes[20,21]when adsorbed as monolayers on particles or surfaces. The ability to use nanochannels to organize molecules in end to end excitonic arrangements provides a challenge for both molecular and material design contributing to a field of great current interest. The possibility to vary the structure of the molecule by inserting spacer groups[38] on either end may provide a method to tune interactions as desired. Studies into determining the coherence length of the excitons, and their relation to the loading are questions posed for further investigation. Finally, the implications that such interactions have on the dynamics of energy transfer and migration, in mixed donor−acceptor zeolites, may further help the understanding of artificial antennae systems.[5]

Acknowledgment. M.B. thanks the Alexander von Humboldt Foundation for Postdoctoral funding. The collaboration between Westfälische Wilhelms-Universität Münster and the MESA$^+$ Institute for Nanotechnology was supported by the FP6 Network of Excellence Frontiers under contract number NMP4-CT-2004-500328 FRONTIERS NoE. Support by Westfälische Wilhelms-Universität Münster is gratefully acknowledged.

Supporting Information Available: Single pixel decay traces and fits from the lifetime imaging experiments as well as the corresponding single pixel spectra. This material is available free of charge via the Internet at http://pubs.acs.org.

JA801178P

(36) McRae, E. G.; Kasha, M. In *Physical Progress in Radiation Biology*; Academic Press: New York, 1964.
(37) Davidov, A. S. *Soviet Phys., USPEKHI* **1964**, *530*, 145–178.
(38) Nolde, F.; Pisula, W.; Müller, S.; Kohl, C.; Müllen, K. *Chem. Mater.* **2006**, *18*, 3715–3725.